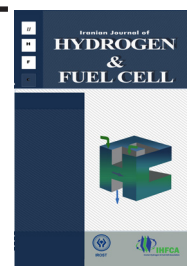


Iranian Journal of Hydrogen & Fuel Cell

IJHFC

Journal homepage://ijhfc.irost.ir



## Investigation of vessels pressure effect on PEM electrolyzer performance by using a new OneDimensional Dynamic Model

Mehdi Jamali Ghahderijani<sup>1</sup>, Fathollah Ommi<sup>2,\*</sup>

<sup>1</sup> PhD candidate, Department of Mechanical Engineering, Aerospace group Tarbiat Modares University, Tehran, Iran

<sup>2</sup> Associated Professor, Department of Mechanical Engineering, Aerospace group Tarbiat Modares University, Tehran, Iran

### Article Information

Article History:

Received:

13 February 2016

Received in revised form:

26 May 2016

Accepted:

08 June 2016

### Keywords

PEM

Dynamic modeling

Finite Volume

Hydrogen production

### Abstract

In recent years the energy shortage and environmental impact from consuming fossil fuels have led to the development of renewable energy source systems. Since these sources are not reliable and are usually time dependent, an energy storing system like hydrogen production is required. In this regard, a PEM electrolyzer can be efficiently used to decompose liquid water into hydrogen and oxygen. Because of the dynamic nature of renewable sources, a dynamic model of a PEM electrolyzer is a necessity for investigating its performance. In this paper, a new one-dimensional dynamic model PEM electrolyzer which solves electrochemical and two phase fluid flow equations at each time step is proposed. The finite volume method with an upwind scheme is used to solve a set of nonlinear partial differential equations of fluid flow for discretization. The obtained algebraic set of equations is implicitly solved to ensure good stability at large time steps as well as low mesh nodes which provide the capability of system level simulation. Storing gas produced by the electrolysis process continuously increases vessels pressure and leads to dynamic behavior of the electrolyzer. This phenomenon is investigated in this research using the proposed model. Results show that although the concentration of produced gas was raised by increasing vessel pressure, the hydrogen concentration was essentially constant along the electrolyzer on the cathode side. It was also observed that increasing vessel pressure results in high power consumption. However, when the pressure on the anode side reaches the moderate level the water mass flow rate can be reduced, which causes a reduction in pump energy consumption.

## 1. Introduction

Energy use is directly linked to well-being and prosperity across the world. Meeting the growing demand for energy in a safe and environmentally responsible manner is an important challenge. A key

driver of energy demand is the human desire to sustain and improve ourselves, our families, and our communities. There are around seven billion people on Earth and population growth will likely lead to an increase in energy demand. Meeting this demand depends on the adequacy of energy resources.

\*Corresponding Author's Tel: +989121324767 Fax: 88269296  
E-mail address: fommi@modares.ac.ir

Moreover, increasing population and economic development in many countries have serious implications for the environment because energy generation processes (e.g., generation of electricity, heating, cooling, and shaft work for transportation and other applications) emit pollutants, many of which are harmful to ecosystems. Burning fossil fuels result in the release of large amounts of greenhouse gases, particularly carbon dioxide [1]. The search for ways to reduce global CO<sub>2</sub> and investigation of non-emission sustainable technologies has substantially increased in recent years. Among the various renewable energy sources, hydrogen as an energy carrier is expected to play a major role in the future of the energy market in addition to the more popularly known solar and wind energy [1]. Water electrolysis efficiently converts clean energy sources into hydrogen, and in this field it is the most mature technology for use in the near future [2]. Electrolyzers are unique devices producing pure hydrogen and oxygen which can then be used for applications such as fuel for hydrogen cars or as an energy storage medium. They can be widely distributed and rated to meet the hydrogen and oxygen requirements of different users such as units for individuals, renewable energy systems, fueling stations and industrial applications [3].

Water electrolysis using PEM electrolyzers is one of the most applicable and efficient method and many studies have focused on state-of-the-art technologies to make it widely cost effective for different applications. In comparison to other technologies, the PEM electrolyzer has several advantages such as higher efficiency, higher current density toleration, pure gas production and safer operation due to the nonhazardous liquid electrolyte. PEM electrolyzers can independently produce high pressure hydrogen up to 130 bar [4] which is beneficial from an economic point of view [2, 5-8].

Electrolyzer modeling has been a subject of much research, and several thermodynamic models, from simple to more sophisticated, have been presented. In this regard, Görgün [3] developed a dynamic model based on conservation of mole balance at the anode and cathode. Dale et al. [9] presented a semi practical

model and considered temperature dependency of reversible voltage. They used a curve-fitting method for fitting the experimental data and determining model parameters. Santarelli et al. [5] investigated the effect of temperature, pressure and feed water flow rate on electrolyzer performance using a regression model. Marangio et al. [10] proposed a theoretical model of an electrolyzer system consisting of activation, concentration and ohmic over-potentials. Awasthi et al. [11] developed a dynamic model in MATLAB/Simulink with the ability to investigate the effects of various operating conditions and electrolyzer components. Lee et al. [12] represented a dynamic model of PEM electrolyzer for regenerative fuel cell applications. They investigated the effects of temperature and mass flow rate and validated their model with experimental data. Kim et al. [1] developed a one-dimensional dynamic model of a high-pressure PEM water electrolyzer. Water transport, gas permeation, gas volume variation in anode/cathode channels, gas compressibility, and water vaporization were considered in their model.

Although the necessity of distributed parameter models are suggested in the literature [10, 13], most proposed models are zero dimensional [1]. In this paper, a new one dimensional (1D) dynamic model which solves electrochemical and two phase fluid flow governing equations at each time step along electrolyzer length is proposed. In contrast to the Kim et al.'s [1] model, in the proposed model the momentum equation is solved which leads to a smoother property distribution of the results as well as better stability behavior. Since filling the vessel with the gas produced from water electrolysis makes the electrolyzer behave dynamically, the proposed model is used to investigate electrolyzer performance in these conditions. The vessel pressure effects on the electrolyzer performance and flow field properties are rarely investigated. Görgün [3] developed a dynamic zero dimensional model in which the hydrogen vessel is considered, but his work doesn't present any information on flow properties distribution inside the electrolyzer cell. In this study it is assumed that the produced gases are directed to their vessels which lead

to a continuous vessels pressure increase. The electrolyzer performance parameters (such as efficiency, power consumption) and flow field properties (such as water concentration ... (include 3 properties, to balance the 3 parameters)) under this condition are presented.

## 2. Electrolyzer Modeling

Fig. 1. shows the schematic of a PEM water electrolyzer in which water from the anode channel diffuses to the MEA and then decomposed to protons and oxygen. Protons migrate through the membrane and compound with the electrons supplied from the DC source to produce hydrogen in the cathode electrode. The electrolyzer cell is divided into three segments namely the anode channel, cathode channel and membrane electrode assembly (MEA). These segments are also split into some arbitrary equal control volumes along the electrolyzer length. Because of the coupling nature of the governing equations, these control volumes should be co-directional along the width of the electrolyzer. Governing equations which will be described in the next subsections should be solved at each of these control volumes.

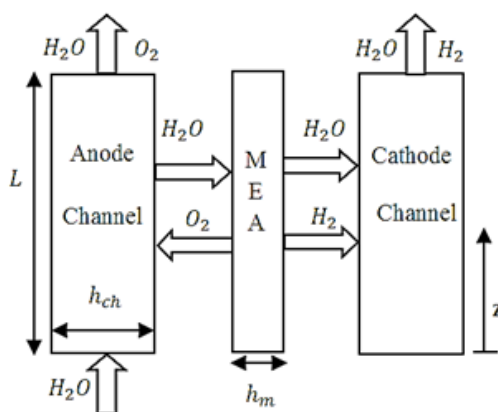


Fig.1. Schematic of a PEM electrolyzer cell.

### 2.1. Electrochemical equations

The voltage required to overcome the water molecule link in the PEM cell is given by:

$$V = E + \eta_{ohm} + \eta_{ac,a} + \eta_{ac,c} \quad (1)$$

Where  $V$  is the electrolyzer voltage and  $\eta_{ohm}$ ,  $\eta_{ac,a}$  and  $\eta_{ac,c}$  are ohmic, anode activation and cathode activation overpotentials, respectively.  $E$  is the open circuit voltage which can be determined from the Nernst equation below [14]:

$$E = E_0 + \frac{RT_{el}}{2F} \left[ \ln \left( \frac{P_{H_2} P_{O_2}^{\frac{1}{2}}}{a_{H_2O}} \right) \right] \quad (2)$$

where  $E_0$  is the standard potential,  $R$  is the gas universal constant,  $T_{el}$  is the cell temperature and  $a_{H_2O}$  is the activity of water between the anode and electrode, assumed equal to 1, for the liquid state. The standard potential is calculated from by [14]:

$$E_0 = \frac{\Delta G_f}{2F} \quad (3)$$

where  $\Delta G_f$  is the Gibbs free energy of formation. Ohmic overpotential in the PEM electrolyzer occurs due to electrical resistance of the cell against the electrical current and membrane resistance against proton migration. This over-potential can be formulated as below [1]:

$$\eta_{ohm} = ir_e + h_m \frac{i}{\sigma_m} \quad (4)$$

In Eq. 4.  $r_e$ ,  $h_m$  and  $\sigma_m$  are the cell electrical resistance, the membrane thickness and the conductivity of membrane, respectively. Here, we assumed that electrodes are perfect conductors so their voltage was constant [1]. Membrane conductivity depends on water content and temperature of the membrane which can be estimated from the practical equation below [10].

$$\sigma_m = [0.005139\lambda_m - 0.00326] \exp \left[ 1268 \left( \frac{1}{303} - \frac{1}{T_m} \right) \right] \quad (5)$$

Activation over-potential is obtained from a simplified form of the Butler-Volmer equation [10]:

$$\eta_{act,a} = \frac{RT_a}{2F} \operatorname{arcsinh} \left( \frac{i}{2i_{0,a}} \right) \quad (6)$$

$$\eta_{act,c} = \frac{2RT_c}{F} \operatorname{arcsinh} \left( \frac{i}{2i_{0,c}} \right) \quad (7)$$

$F$  is the Faraday constant, while  $i_{0,a}$  and  $i_{0,c}$  are the exchange current densities at the anode and cathode, respectively. Production/destruction rates of species are given by Faraday's law:

$$\dot{n}_{H_2} = \frac{i}{2F} \quad (8)$$

$$\dot{n}_{O_2} = \frac{i}{4F} \quad (9)$$

$$\dot{n}_{H_2O} = \frac{i}{2F} \quad (10)$$

## 2.2. Water transport mechanisms

Three major water transport mechanisms exist in PEM electrolyzer cells: the concentration gradient, pressure gradient and electro-osmotic drag. Among them, the last one has the most important role in water transportation [1, 10-11]. Water transport due to concentration gradient can be obtained using Fick's law [15]:

$$\dot{n}_d = D_w \frac{C_{w,a} - C_{w,c}}{h_m} \quad (11)$$

where  $D_w$  is the water diffusion coefficient in the membrane.  $C_{w,c}$  and  $C_{w,a}$  are water concentrations at the cathode side and anode side, respectively, and  $h_m$  is the membrane thickness. Water transport due to pressure gradient can be calculated using Darcy's law [15]:

$$\dot{n}_p = \left( \frac{K \rho_w}{\mu_w M_w} \right) \frac{P_c - P_a}{h_m} \quad (12)$$

where  $K$  is the Darcy constant, and  $\rho_w$  and  $\mu_w$  are the density and dynamic viscosity of water, respectively.  $P_c$  and  $P_a$  represent the pressure at the cathode and anode sides of the cell. Water transport due to electro-osmotic drag is proportional to current density and is given by [1]:

$$\dot{n}_{eo} = n_{ed} \frac{i}{F} \quad (13)$$

The constant  $n_{ed}$  depends on the pressure, temperature and current density. Medina and Santarelli (13) suggested a linear regression model for estimation of the electro-osmotic drag coefficient:

$$n_{ed} = 0.0252P_c - 1.9073i + 0.0189T_m - 2.7892 \quad (14)$$

## 2.3. Fluid Flow in Channels

Liquid water enters into the anode channel and diffuses into the MEA and then reaches the cathode channel by diffusion. In the same manner, gas produced in the electrodes diffuses to both channels. As a result, the fluid flow in the channels should be treated as a two phase flow. Considering the dynamic aspects, an unsteady homogenous two phase flow model was used to simulate fluid flow behavior in the channels. The mass transport phenomenon which occurs through the membrane is considered as a source term in the governing equations [16]:

$$\frac{\partial \alpha_{gk} \rho_{gk}}{\partial t} + \frac{\partial \alpha_{gk} \rho_{gk} u_k}{\partial z} = \dot{n}_{gk} \quad (15)$$

$$\frac{\partial \alpha_{lk} \rho_{lk}}{\partial t} + \frac{\partial \alpha_{lk} \rho_{lk} u_k}{\partial z} = \dot{n}_{lk} \quad k = a, c \quad (16)$$

$$\frac{\partial \alpha_{gk} \rho_{gk} u_k}{\partial t} + \frac{\partial \alpha_{gk} \rho_{gk} u_k^2}{\partial z} + \alpha_{gk} \frac{\partial P_k}{\partial z} = 0 \quad (17)$$

In Eqs.1-3  $\alpha$  is the void fraction,  $\rho$  is the partial density,  $u$  is the flow velocity and  $\dot{n}$  represents the mass flow rate into/from the channel with subscripts l/g for liquid/gas and  $k$  for channel (anode a /cathode c), respectively.

## 2.4. Vessels

The gas produced is stored by conducting it into the vessels after water separation. Gas accumulation causes the vessel pressure to rise which affects flow characteristics. In this regard, the mass flow rate of

gas production is calculated by Eq.18, then using the constant mass flow rate assumption and the ideal gas law at each time step the vessel pressure is obtained by Eq.19:

$$\dot{m}_{gk} = \dot{a}_{gk} \tilde{n}_{gk} u_{gk} w_{ch,k} h_{ch,k} \quad (18)$$

$$P_{v,gk} = \left( \frac{\dot{m}_{gk} R_{gk} T_{vk}}{V_{gk}} \right) dt \quad k = a, c \quad (19)$$

$$P_{v,gk} = \left( \frac{\dot{m}_{gk} R_{gk} T_{vk}}{V_{gk}} \right) dt \quad k = a, c \quad (20)$$

where  $w_{ch}$  and  $h_{ch}$  are the channel width and height, respectively.  $R_{gk}$  represents the gas constant at each channel,  $T_{vk}$  is the vessel temperature and  $V_{gk}$  is the vessels volume. It is also assumed that the vessel temperature is constant throughout the storing process because the process is slow [3].

## 2. 5. Initial and Boundary Condition

Fig.2 shows the boundary conditions used for solving the electrolyzer modeling governing equations. Inlet velocity can be obtained using mass flow rate as well as outlet pressure from the vessel pressure at each time step. Initial conditions could be specified from a homogenous distribution of boundary conditions. However, in the case of void fraction special care must be taken for selecting both inlet and initial boundary condition. Actually, the zero amount of void fraction results in zero gas pressure which leads to infinity open circuit voltage (Eq.2). Thus a small but non zero value (e.g. 0.001) should be assigned to the void fraction as the initial and inlet boundary condition, whereas input water is assumed to be pure.

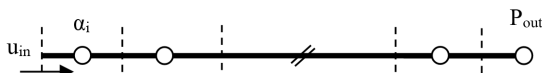


Fig.2. Boundary conditions in electrolyzer modeling.

## 2.6.Solving the governing equations

In order to solve the set of above nonlinear partial differential equations, at first they are discretized using finite volume method with upwind scheme using staggered meshes [17]. The obtained set of nonlinear algebraic equations is implicitly solved by using Newton linearization method [18]. Although the implicit approach requires more computational effort at each time step than explicit approach, it has some advantages which make this approach beneficial from total run time point of view [19]. In fact, in this approach selection of time step is independent of the spatial mesh nodes and the stability of solution is very good. These characteristics allow larger time steps and lower mesh sizes to be implemented which means lower total computational effort to simulate whole system. Fig.3 shows the flowchart of solving procedure of governing equations and the computer code which developed based on proposed model. In this regard, at first the constant parameters which consist of electrolyzer cell geometry, fluid properties and electrochemical constants should be entered to the code. Then according to section 2-5, variables initialization is performed. By solving electrochemical equations (Eq.1-7) and obtaining current density distribution, the species production/destruction rates can be determined. Thereafter using Eqs.11-14 water transport rate which allows to calculate mass flow rate into/from the channel ( $\dot{n}$ ) could be attained. Then the set of nonlinear partial differential equations (Eq.15-17) are discretized and solved which is the most difficult and time consuming step. Finding velocity, void fraction and density of each species at channels allows calculating mass flow rate of gases flowing into the vessels. Using perfect gas law the vessel pressure can be obtained at each time step. The iterations should be continued at new time step and ended when achieving the specified time ( $t_{max}$ ).

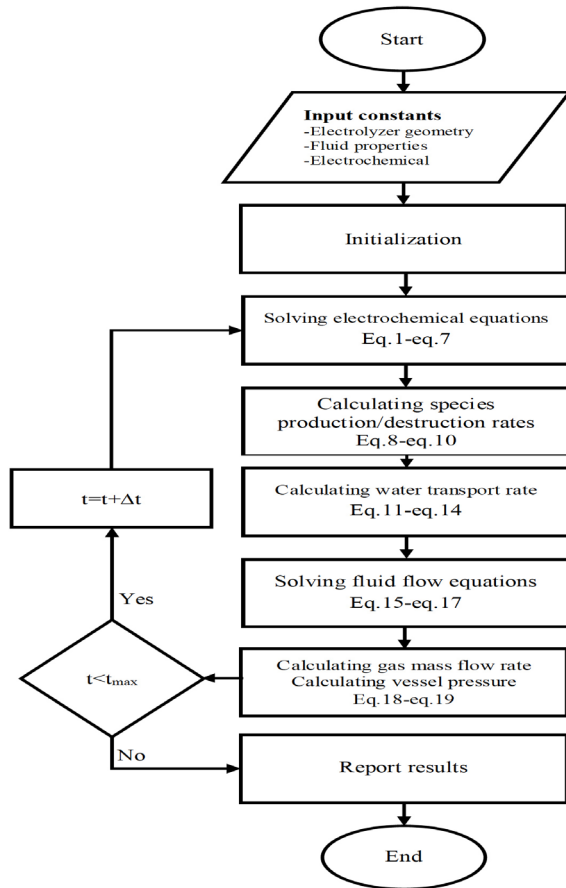


Fig.3. Flowchart of the procedure to solve the proposed model.

## 3. Results and discussion

### 3. 1. Validation

Since the experimentally evaluated flow properties along the length of PEM electrolyzer are so scarce (almost not available), the validation of the proposed model was done using Kim et al.'s [1] model. Table 1 summarizes the data used in the simulation. The steady state properties distribution consisting of water concentration and velocity are shown in Fig.4 and Fig.5. Although results were very close at each node in both models, in the proposed model there was no oscillatory behavior especially in velocity distribution (see Fig.5). This outcome is the result of considering the momentum equation during electrolyzer modeling in the present model rather than the Kim et al. model. The cell performance curve (I-V) of both models is

compared in Fig.6. Since the hydrogen diffusion across the membrane from cathode to the anode side is not considered in the modeling procedure in this paper, the cell voltage is underestimated in the proposed model. In Fig.7 the dynamic response to the current density change is presented for both models. As seen in this figure, the average current density suddenly changed from  $1\text{A}/\text{cm}^2$  to  $1.2\text{A}/\text{cm}^2$  and changed again

Table1: Parameters used in the Validation Process [1]

#### Cell dimensions

Length: 0.3 m, Width: 0.105 m, Area:  $0.0314\text{ m}^2$ ,  
Number of cells: 120, Channel height:  $h_{ch} = 0.003\text{ m}$ ,  
Electrode height:  $h_c = 0.0005\text{ m}$ , Membrane height:  
 $h_m = 0.0002\text{ m}$

#### Constants

Electric resistance:  $r_c = 0.035\text{ m}\Omega$   
Degree of membrane humidification:  $\lambda_m = 25$   
Anode exchange current density:  $i_{oa} = 10^{-6}\text{ A}/\text{m}^2$   
Cathode exchange current density:  $i_{oc} = 10\text{ A}/\text{m}^2$   
Water diffusion coefficient:  $D_w = 1.28 \times 10^{-10}\text{ m}^2/\text{s}$   
Darcy's constant:  $K = 1.58 \times 10^{-18}\text{ m}^2$

#### Nominal operating condition

Current density:  $i_{ave} = 10000\text{ A}/\text{m}^2$   
Pressure at the cathode:  $P_c = 100\text{ bar}$   
Pressure at the anode:  $P_a = 2\text{ bar}$   
Inlet water flow rate:  $Q_{in} = 100\text{ l}/\text{min}$   
Inlet water temperature:  $T_{in} = 55^\circ\text{C}$

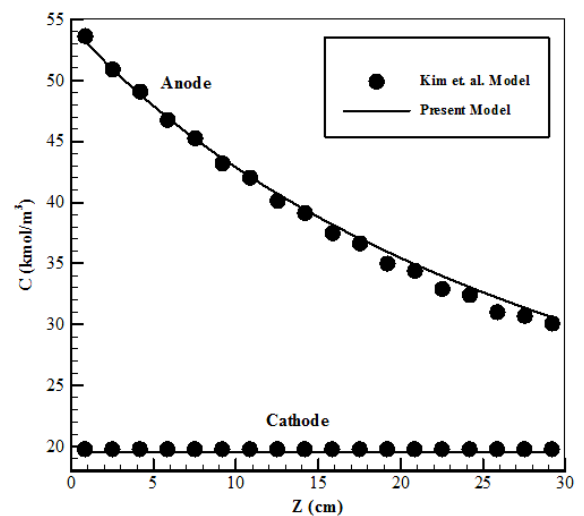


Fig.4. Distribution of water concentration along the electrolyzer length.

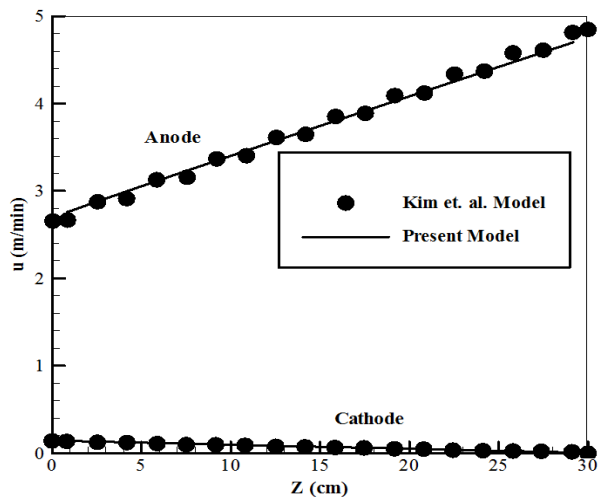


Fig.5. Velocity distribution along the electrolyzer length.

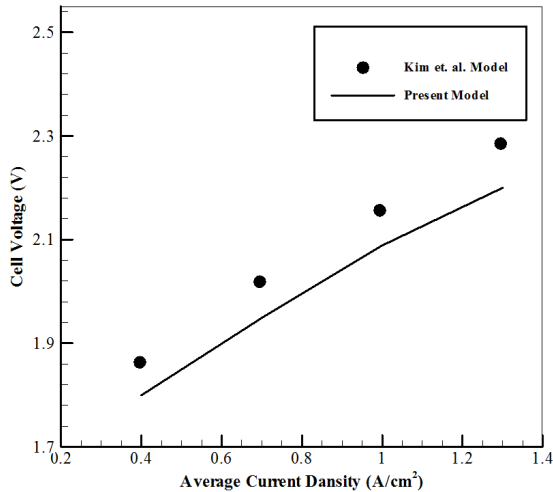


Fig.6. Performance curve of the electrolyzer.

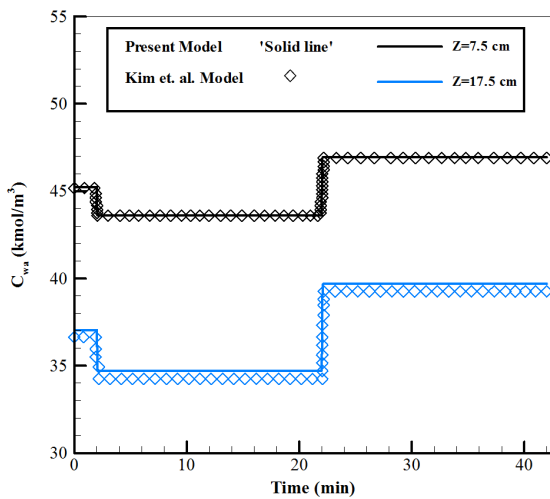


Fig.7. Dynamic response to the current density change.

to  $0.8\text{A}/\text{cm}^2$  at time  $t=2\text{min}$  and  $22\text{min}$ , respectively. The water concentration at two cross sections ( $z=7.5$  and  $17.5\text{cm}$ ) at both anode and cathode sides was compared and were very close in both models. After the validation, the effect of mesh and time step size was performed. Fig.8 shows the effect of using various mesh nodes, and Fig.9 illustrates the effect of time step size. As illustrated, the results confirm the capability of this model for large time step size and low mesh nodes.

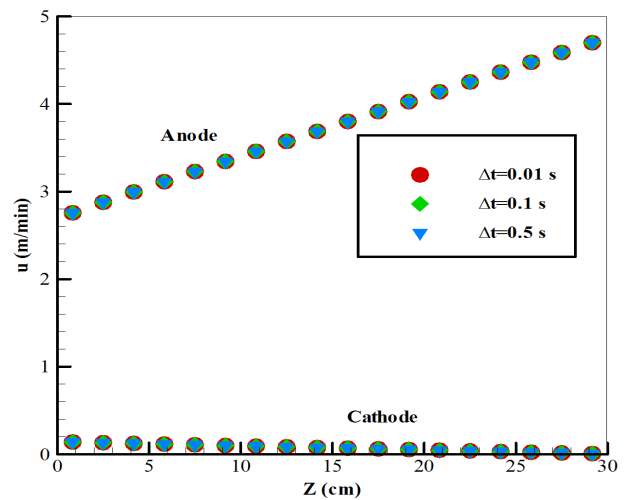


Fig.8. Effect of selecting various time step on the velocity distribution at  $n=18$  mesh nodes.

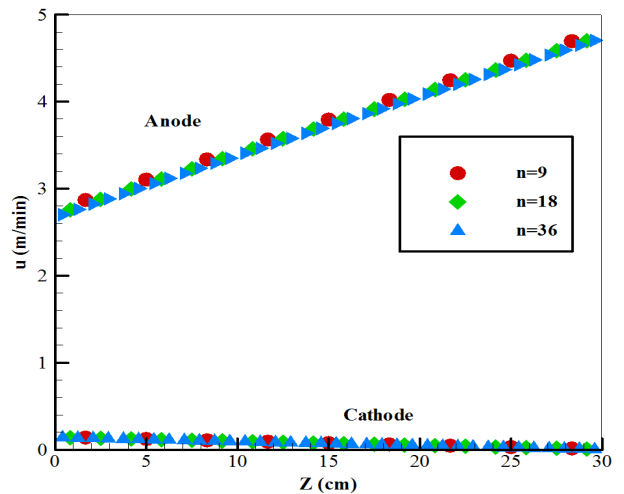


Fig.9. Effect of various number of mesh node on the velocity distribution at  $\Delta t=0.01\text{s}$ .

### 3. 2. Vessel filling and its effect on the cell performance

One advantage of PEM electrolyzers is the production of high pressure hydrogen without any compressing equipment. During vessel filling the pressure is going to rise which leads to dynamic behavior of the electrolyzer. Although vessel filling affects cell performance, this phenomenon is rarely investigated [3]. To explore the electrolyzer cell performance during vessel filling, two scenarios were considered. Like most hydrogen production cases, in the first scenario the produced hydrogen is stored in the vessel while the produced oxygen is evacuated to the atmosphere. Sometimes the pressure of the anode side, where oxygen is produced, also increased. When there is very high pressure hydrogen production without using any compressor, the pressure of the anode side should also increase to prevent membrane crack and system failure. Moreover, when the produced oxygen is considered as a valuable by product and stored, the anode pressure shows dynamic behavior, too. In this section, in the second scenario it is supposed that both hydrogen and oxygen are valuable and conducted to the vessels.

In both scenarios it was assumed that the electrolyzer was in the steady state condition with an anode and cathode pressure equal to 1 bar, then hydrogen/oxygen began to be stored in the vessels until it reached a maximum pressure (100 bar). The current density was supposed to be constant (1 A/cm<sup>2</sup>), so the cell voltage and power consumption increased during the vessel filling (see Fig.10). Since the required time for the filling of vessels was related to the vessel volume as well as the number of electrolyzer cells, for the sake of generality the results were presented against vessel pressure  $P_v$ . To evaluate the performance of the system, system efficiency  $\eta_{sys}$  was defined by Eq.20 [1]:

$$\eta_{sys} = \frac{HHV \text{ of produced Hydrogen}}{i_{ave} \cdot V \cdot W_{ch} \cdot L} \quad (20)$$

where HHV is the higher heating value of hydrogen. As it can be seen in Fig.10, during vessel filling the efficiency of the electrolyzer cell declined, whereas

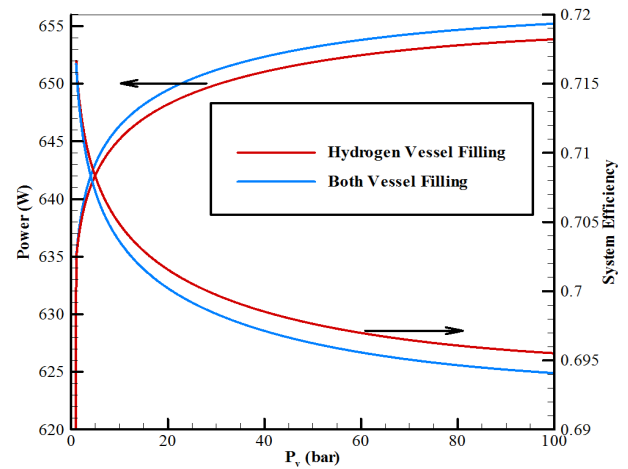


Fig.10. Power consumption and system efficiency during vessel filling.

in contrast the power consumption rose. In addition, the efficiency profile of the second scenario is lower than the first, which means filling both vessels results in lower system efficiency. From the Nernst equation (Eq.2) we found that the higher the gas products pressure, the higher the cell voltage is needed which means higher power consumption at constant average current density. Since the hydrogen production rate is only related to current density (Eq.8). According to Eq.20, more power consumption leads to lower system efficiency in the second scenario.

The water concentration at the cathode side rises in both scenarios and has almost a constant distribution along the electrolyzer length (see Figs.11-12). Since in the first scenario oxygen vessel pressure is constant, there is no change in the water concentration at the anode side during hydrogen vessel filling. However, water concentration declines along the cell length because of water consumption and water transportation to the cathode side. Fig.12 shows that in the second scenario as the vessel pressure raises the water concentration at the anode side, it increases until it reaches a constant value. Oxygen and hydrogen concentration for both scenarios are shown in Fig.13 and Fig.14. As can be seen in these figures, the hydrogen concentration rises as vessel pressure increases. It is also nearly constant along the cell length. At the anode side oxygen concentration increases along the electrolyzer cell (see Fig.13) due to oxygen production. However, in

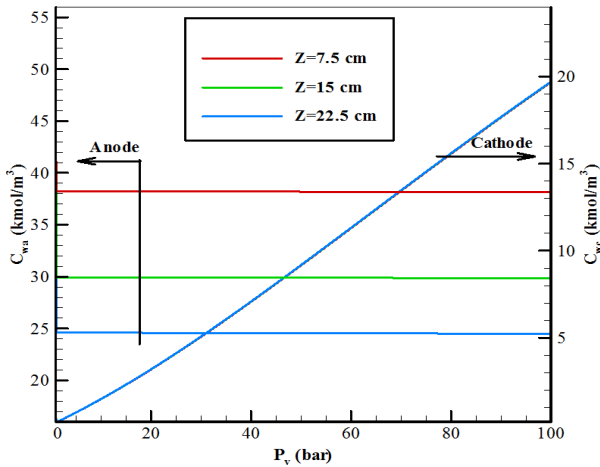


Fig.11: Water concentration distribution at anode and cathode sides during hydrogen vessel filling.

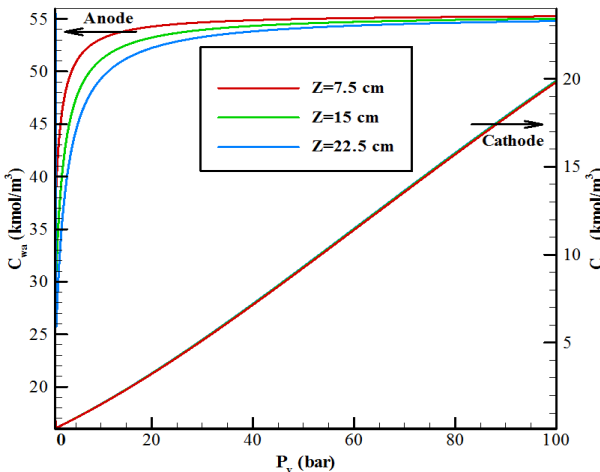


Fig.12: Water concentration distribution at anode and cathode sides during the filling of both vessels.

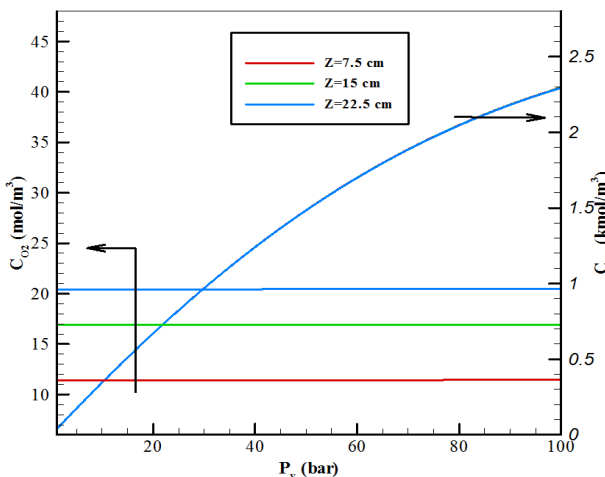


Fig.13: Hydrogen and oxygen concentration distribution at anode and cathode sides during the filling of the hydrogen vessels.

the second scenario the oxygen concentration at each point along the cell length is slowly increased after a sharp increment occurring at low and moderate vessel pressure (see Fig.14). In fact, increasing the anode pressure has little effect on the liquid water density, unlike oxygen as an ideal gas. Therefore, the occupied volume of oxygen declines which leads to increases in the water concentration to values near pure water concentration (see Fig.12). This is an important outcome for system design and optimization. In fact, the water flow rate in the water electrolyzer is much higher than water consumption to prevent membrane dryness. According to the above discussion, it was found that when vessel pressure reaches moderate levels it is possible to decrease inlet mass flow rate and subsequently decrease pump power consumption without any issues regarding membrane dryness. Since species concentration is influenced by vessels pressure during their filling, the velocity distribution in the channels is also affected. Fig.15 shows the velocity distribution at anode and cathode sides at some selected pressures during vessel filling in the second scenario. As can be seen, the velocity distribution at both sides decreases and tends to be flat when the vessels pressure increases. This phenomenon is observed because of the increasing gas concentration (as discussed above) and exposing the electrolyzer to a constant average current density. Since the gas production rate is dependent on the current density

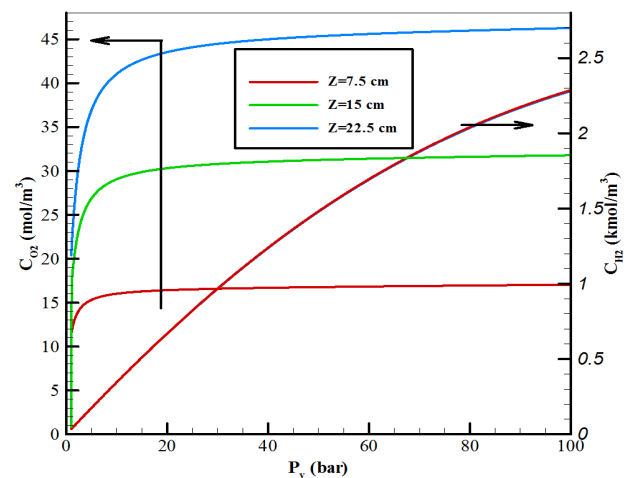
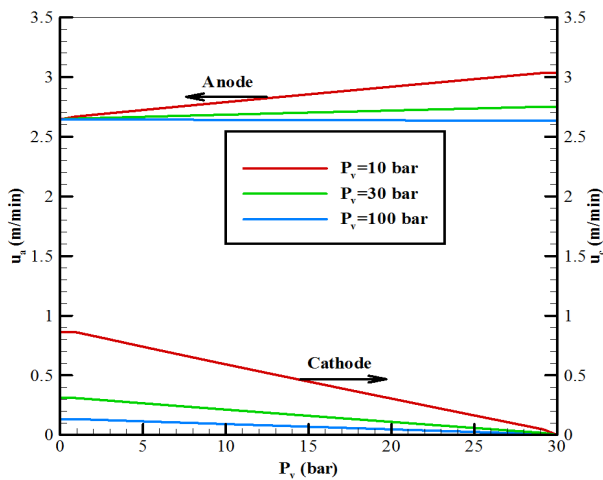


Fig.14: Hydrogen and oxygen concentration distribution at anode and cathode sides during the filling of both vessels.



**Fig.15: Velocity distribution at anode and cathode sides at some selected pressure during the filling of both vessels.**

(Eq.8-9), it remains fairly constant. Therefore, the flow velocity is forced lower when vessel pressure is raised.

## 4. Conclusion

In this paper, a new one dimensional dynamic model of a PEM electrolyzer capable of accurately predicting flow properties at both steady and dynamic state is proposed. In this model, electrochemical and unsteady homogenous two phase fluid flow governing equations are solved at each control volume along the electrolyzer cell length. In contrast to the Kim et al. model, solving momentum equation using the finite volume method in an implicit manner allows this model to present a smoother flow properties distribution and enjoy great stability over larger time and spatial step sizes. Therefore, the proposed model can be used for system level design and optimization as well as for detail study and research. By using the proposed model, the effect of vessel pressure during vessel filling was investigated. The results illustrated that an increase in vessel pressure results in increased power consumption and decreased efficiency especially when both vessels are filled. Results also reveal that although the power consumption is higher during both vessels filling, it is possible to reduce inlet

water mass flow rate at moderate pressure which leads to lower pump power consumption.

## 5. References

- [1] Kim H., Park M. and Lee K. S., "One-dimensional dynamic modeling of a highpressure water electrolysis system for hydrogen production", *Int J Hydrogen Energy*, 2013, 38: 2596.
- [2] Marangio F., Pagani M., Santarelli M. and Cali M., "Concept of a high pressure PEM electrolyser prototype", *Int J Hydrogen Energy*, 2011, 36: 7807.
- [3] Gorgun H., "Dynamic modeling of a proton exchange membrane (PEM) electrolyzer", *Int J Hydrogen Energy*, 2006, 31: 29.
- [4] Grigoriev, S.A., Porembskiy V.I., Korobtsev S.V., Fateev V.N., Auaprêtre F. and Millet P., "High-pressure PEM water electrolysis and corresponding safety issues", *Int J Hydrogen Energy*, 2011, 36: 2721.
- [5] Santarelli M., Medina P. and Cali M., "Fitting regression model and experimental validation for a high pressure PEM electrolyzer", *Int J Hydrogen Energy*, 2009, 34: 2519.
- [6] Roy A., Watson S. and Infield D., "Comparison of electrical energy efficiency of atmospheric and high-pressure electrolyzers", *Int J Hydrogen Energy*, 2006, 31: 1964.
- [7] Onda K., Takahiro K., Kikuo H. and Kohei I., "Prediction of production power for high-pressure hydrogen by high-pressure water electrolysis", *Journal of Power Sources*, 2004, 132: 64.
- [8] Todd D., Schwager M. and Mercida W., "Thermodynamics of high-temperature, high-pressure water electrolysis", *Journal of Power Sources*, 2014, 269: 424.
- [9] Dale N.V., Mann M.D. and Salehfar H., "Semi-empirical model based on thermodynamic principles for determining

6 kW proton exchange membrane electrolyzer stack characteristics", *Journal of Power Sources*, 2008, 185: 1348

[10] Marangio, F., Santarelli, M. and Cali, M., "Theoretical model and experimental analysis of a high pressure PEM water electrolyzer for hydrogen production", *Int J Hydrogen Energy*, 2009, 34: 1143.

[11] Awasthi, A., Scott K. and Basu S., "Dynamic modeling and simulation of a proton exchange membrane electrolyzer for hydrogen production", *Int J Hydrogen Energy*, 2011, 36: 14779.

[12] Lee B. Park K. and Man Kim H. "Dynamic Simulation of PEM Water Electrolysis and Comparison with Experiments", *Int. J. Electrochem*, 2013, 8: 235.

[13] Medina P. and Santarelli M., "Analysis of water transport in a high pressure PEM electrolyzer", *International Journal of Hydrogen Energy*, 2010, 35: 5173.

[14] Larminie J. and Dicks A., 2nd ed., *Fuel cell systems explained*, John Wiley & Sons, 2003.

[15] Bird R. B., Stewart W. E. and Lightfoot E. N., 2nd ed., *Transport Phenomena*, John Wiley & Sons, 2007.

[16] Bertola V., 1st ed., *Modelling and Experimentation in Two-Phase Flow*, Springer-Verlag Wien GmbH, 2014.

[17] Versteeg H. K., and Malalasekera W., 2nd ed., *Introduction to Computational Fluid Dynamics: The Finite Volume Method*, Pearson Education Limited, 2007.

[18] Rheinboldt W. C. 2nd ed., *Methods for Solving Systems of Nonlinear Equations*, SIAM, 1998.

[19] Abbaspour M., Chapman K. S. and Glasgow L., "Transient modeling of non-isothermal, dispersed two-phase flow in natural gas pipelines", *Applied Mathematical Modelling*, 2010, 34, 495.